Experimental Demonstration of Single Sideband Modulation Utilizing Monolithic Integrated Injection Locked DFB Laser

Yunshan Zhang, Bocheng Yuan, Lianyan Li, Jie Zeng, Zijun Shang, Jilin Zheng, Zuye Lu, Shijian Guan, Xing Zhang, Rulei Xiao, Tao Fang, Yuechun Shi, Hui Zou, Jianping Shen, and Xiangfei Chen, *Senior Member, IEEE*

***Abstract*—Single sideband (SSB) modulation based on a monolithic integrated optically injection-locked (MOIL) DFB laser is demonstrated experimentally. To our knowledge, this is the first time to realize SSB modulation utilizing a MOIL DFB laser. Tunable SSB signals with large lower-to-upper sideband power ratios are achieved by changing the bias currents of the MOIL DFB laser. The largest lower-to-upper sideband power ratio is measured to be 24.4 dB, which is very useful for improving the transmission performance of a radio-over-fiber link. Due to the generated SSB modulation, the fiber transmission response is flattened significantly and a signal of 25 GHz is transmitted through 85-km fiber without being affected by the fiber chromatic dispersion. 20 MSymbol/s 32-QAM signals with subcarriers of 21 GHz, 23 GHz, and 25 GHz are also transmitted by the proposed SSB modulation link, and both the error vector magnitude (EVM) and the bit error rate (BER) of the link are improved distinctly. The proposed method can effectively suppress the fiber chromatic dispersion.**

***Index Terms*—Fiber chromatic dispersion, optical injection-locked DFB laser, photonic integration, single sideband modulation (SSB).**

Manuscript received August 5, 2019; revised October 29, 2019; accepted December 4, 2019. Date of publication December 16, 2019; date of current version April 1, 2020. This work was supported in part by the Chinese National Key Basic Research Special Fund under Grant 2017YFA0206401, in part by the National Natural Science Foundation of China under Grants 61974165 and 61673393, in part by the Jiangsu Science and Technology Project under Grant BE2017003-2, in part by the Natural Science Foundation of Jiangsu Province for the Youth under Grant BK20160907, in part by the Open Foundation of Research Center of Optical Communications Engineering & Technology, Jiangsu Province under Grant ZXF20170302 and ZXF20170102, and in part by the Suzhou Technological Innovation of Key Industries under Grant SYG201844. *(Corresponding author: Jilin Zheng.)*

Y. Zhang, B. Yuan, L. Li, Z. Shang, H. Zou, and J. Shen are with the College of Electronic and Optical Engineering & College of Microelectronics, Nanjing University of Posts and Telecommunications, Nanjing 210023, China (e-mail: yszhang@njupt.edu.cn; 931141124@qq.com; lilianyan@njupt.edu.cn; zjs13485310000@163.com; huizou@njupt.edu.cn; jianpingshen@njupt.edu.cn).

J. Zeng, Z. Lu, S. Guan, R. Xiao, T. Fang, and X. Chen are with the College of Engineering and Applied Sciences, Nanjing University, Nanjing 210093, China (e-mail: 549720438@qq.com; 798005027@qq.com; 965872540@qq.com; rolray@163.com; fangt@nju.edu.cn; chenxf@nju.edu.cn).

Y. Shi is with the College of Engineering and Applied Sciences, Nanjing University, Nanjing 210093, China, and also with the High-Tech Institute, Nanjing University, Suzhou 215123, China (e-mail: shiyc@nju.edu.cn).

J. Zheng is with the College of Communications Engineering, PLA Army Engineering University, Nanjing 210007, China (e-mail: zhengjilinjs@126.com).

X. Zhang is with the Changchun Institute of Optics, Fine Mechanics and Physics, Chinese Academy of Science, Changchun 130033, China (e-mail: zhangx@ciomp.ac.cn).

Color versions of one or more of the figures in this article are available online at http://ieeexplore.ieee.org.

Digital Object Identifier 10.1109/JLT.2019.2959796

I. Introduction

RADIO-OVER-FIBER (ROF) technology has gained great interests in recent years due to its promising applications in wideband access networks and microwave photonic radar. Standard modulation method generates two signal sidebands on both sides of the optical carrier. Consequently, the chromatic dispersion of the standard single mode fiber (SMF) results in serious degradation of the received signal in ROF systems. The single-sideband modulation (SSB) technique has been proposed to solve this problem and several methods have been developed to realize SSB modulation. SSB signals can be obtained utilizing Mach-Zehnder modulators combining with narrow optical filter (i.e., by suppressing one of the two sidebands) [1], [2]. Stimulated Brillouin scattering effect in fiber can be used to generate SSB signals, in which only one modulation sideband is amplified [3], [4]. Direct SSB modulation can also be obtained using an optically injection-locked semiconductor laser [5], [6]. All the above-mentioned methods are realized by several separately packaged devices. Due to the use of discrete devices, the SSB modulation systems are very complicated and their portability is limited. Monolithic integrated optically injection-locked (MOIL) semiconductor lasers with advantages of small size, low power consumption and low nonlinear distortion have been developed for ROF applications [7]–[9]. However, it is challenging for MOIL semiconductor lasers to realize SSB modulation, which requires large injection ratio. Due to the lack of optical isolator between the master laser (ML) and the slave laser (SL), various optical nonlinear effects, including the mutually stable locking, period-1 oscillation, frequency locking, quasi-periodicity, four-wave mixing and chaos, can be observed under strong injection state [10]–[13]. All the optical nonlinear effects may deteriorate the SSB modulation significantly.

In this letter, we experimentally demonstrate the direct SSB modulation based on a MOIL DFB laser which has been previously reported [14]. To our knowledge, this is the first time that the SSB modulation is obtained utilizing a MOIL laser chip.

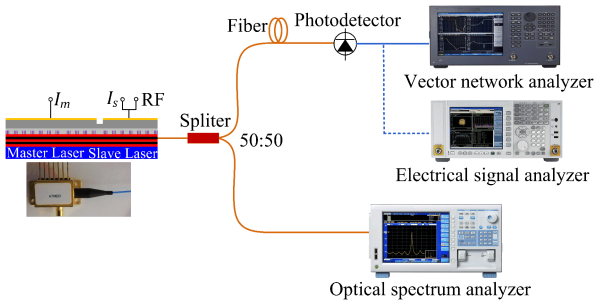

Fig. 1. The experimental setup of the SSB system. Inset is the photograph of the packaged MOIL DFB laser. ML: Master Laser, SL: Slave laser, PD: Photodetector, VNA: Vector Network Analyzer, ESA: Electrical Signal Analyzer, and OSA: Optical Spectrum Analyzer.

The MOIL DFB laser is realized utilizing the side-mode injection locking method which can suppress the nonlinear effects between the integrated ML and SL [15], [16]. Consequently, the MOIL DFB laser achieves SSB modulation at different frequencies in a large injection-locked range without being influenced by the nonlinear effects. By tuning the bias current of the MOIL DFB laser, the maximum lower-to-upper sideband power ratios (P_{lsp}/P_{usp}) achieve to be 20.3 dB, 24.4 dB and 24.3 dB for 21GHz, 23 GHz and 25 GHz respectively, which are no less than the results obtained by separate devices [5], [6]. The SSB fiber transmission response is measured and normalized to the back-to-back frequency response of the MOIL DFB laser. In the free-running state, the fiber transmission response of the laser shows several pronounced dips and the largest one is more than 16.20 dB. While the transmission response curves are flattened in the injection-locked case and the largest dip is reduced to 7.1 dB. Furthermore, the SSB modulation properties of the MOIL DFB laser are investigated by a simple ROF link. 20 MSymbol/s 32-QAM signals with subcarriers of 21 GHz, 23 GHz and 25 GHz are transmitted through a 25-km SMF. The error vector magnitude (EVM) of the link is improved distinctly by the SSB modulation and bit error rate (BER) less than 10^{-13} is achieved.

II. Experimental Setup and Principle

A. Design of the Laser Chip and Experimental Setup

The schematic of the experimental setup is shown in Fig. 1. The MOIL DFB laser is an integrated two-section DFB laser. One section is the ML and the other one is the SL (SL). The lengths of the two sections are 450 μm and 350 μm respectively. the currents of the ML and SL are labeled as I_m and I_s. The radio frequency (RF) signal is injected into the SL section via a Bias Tee. The epitaxial structure of the MOIL DFB laser is grown by a conventional two-stage metal-organic chemical vapor deposition (MOCVD). An n-InP buffer layer, an n-InAlGaAs lower optical confinement layer, an InAlGaAs multiple-quantum-well (MQW) structure, a p-InGaAsP upper optical confinement layer and a p-InGaAsP grating layer are successively grown on an n-InP substrate in the first epitaxial growth. In order to obtain a strong grating, the thickness of the grating layer is set at 50 nm. Then the sampled grating is fabricated by a conventional holographic exposure combining with conventional photolithography. After the forming of the sampled grating, a p-InP cladding layer and a p-InGaAs contact layer are successively regrown over the entire structure. The devices are realized by processing ridge wave guides, opening p-metal contact windows, followed by metallization. In addition, in order to obtain high electrical isolation, a small area of the highly p-doped InGaAs contact layer between the two sections is removed by etching. The resistance between the ML and SL is more than 3 kΩ. Finally, AR coatings with reflectivity less than 1% are deposited on both facets to suppress the Fabry-Perot modes of the lasers. More details about the MOIL DFB laser can be found in [14].

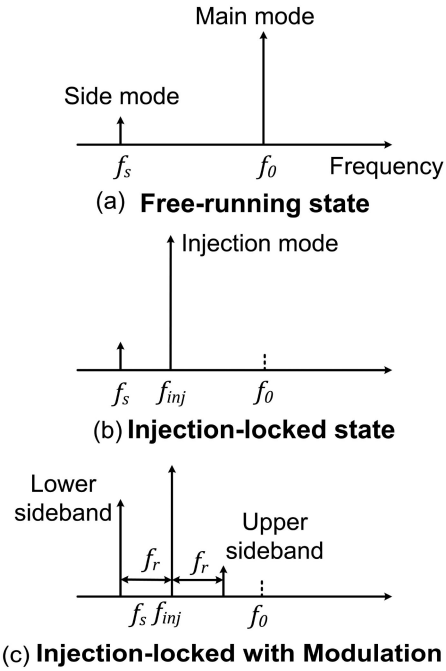

Fig. 2. Optical spectra illustrating SSB modulation based on a MOIL DFB laser. (a) Free-running laser without RF modulation. (b) Injection-locked laser without RF modulation. (c) Injection-locked laser modulated by an RF signal with a modulation frequency of f_r.

The output of the MOIL DFB laser is split into two routes. One route is connected to the optical spectrum analyzer (OSA) to monitor the spectra of the SSB signals. On the other route, a long optical fiber, a high-speed photodetector with bandwidth of 50 GHz, a vector network analyzer (VNA) and an electrical signal analyzer (ESA) are employed to monitor the RF performance of the SSB system.

B. SSB Modulation Principle Using the MOIL DFB Laser

Fig. 2 illustrates the principle of the SSB modulation based on the MOIL DFB laser. In the free-running state, the SL has a main mode and a side mode with frequency of f_0 and f_s respectively. When the MOIL DFB laser is in injection-locked state, the main mode of the SL is suppressed and the output frequency of the MOIL DFB laser is f_{inj} which is defined by the ML. In order to obtain stable injection-locked state, the injection locked mode is designed to be close to the side mode of the

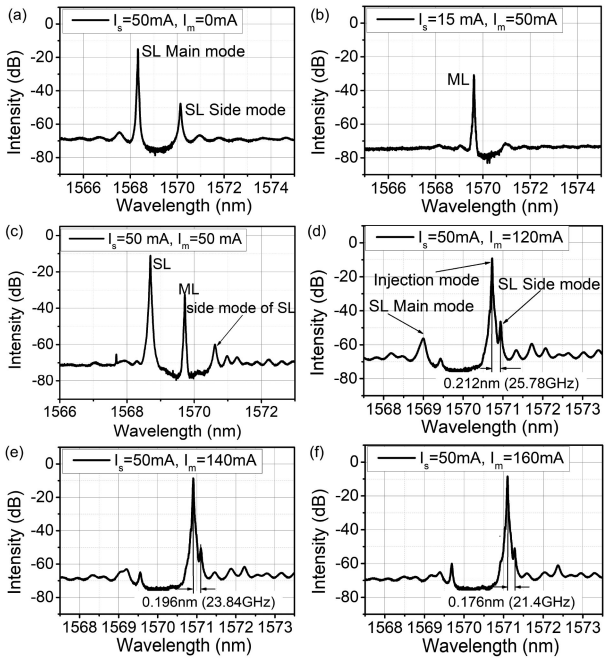

Fig. 3. Measured optical spectra of the MOIL DFB laser with different bias currents. (a) $I_s = 50$ mA, $I_m = 0$ mA, (b) $I_s = 15$ mA, $I_m = 50$ mA, (c) $I_s = 50$ mA, $I_m = 50$ mA, (d) $I_s = 50$ mA, $I_m = 120$ mA, (e) $I_s = 50$ mA, $I_m = 140$ mA, and (f) $I_s = 50$ mA, $I_m = 160$ mA.

SL (i.e., the side-mode injection locking method). When the injection-locked MOIL DFB laser is modulated by a RF signal with a frequency of f_r ($f_r \approx f_{inj} - f_s$), the lower sideband is resonantly amplified by the side mode of the SL and the upper sideband remains unchanged. Consequently, the P_{lsp}/P_{usp} goes to a high value which can be controlled through tuning two important parameters in the MOIL DFB laser, the frequency detuning and the injection ratio. Here, the frequency detuning is defined as the frequency difference between the ML and the side-mode of the SL and the injection ratio is the ratio between the power injected into the SL from the ML and the power of the SL at free running state. In the MOIL DFB laser, both the frequency detuning and the injection ratio are tuned by changing the bias currents of the ML and SL.

III. Experimental Results and Discussion

A. Characteristics of the Injection-Locked MOIL DFB Laser

The injection locking process in the MOIL DFB laser is more complicated due to the lack of optical isolator between the ML and SL [17], [18]. However, the injection locking process can be observed under the condition of monolithic integration if the ML and SL lasers are properly designed [19]–[22]. Firstly, the ML and SL should operate independently, so strong gratings and electrical isolation are required in MOIL laser [23]. Moreover, in order to increase the stable injection locking bandwidth, the side-mode injection technique is utilized [15], [16]. To explain the injection locking process in detail, the performances of the MOIL laser under injection locking state are described in the following.

The measured spectra of the MOIL DFB laser with different I_s and I_m are shown in Fig. 3. It can be seen that when

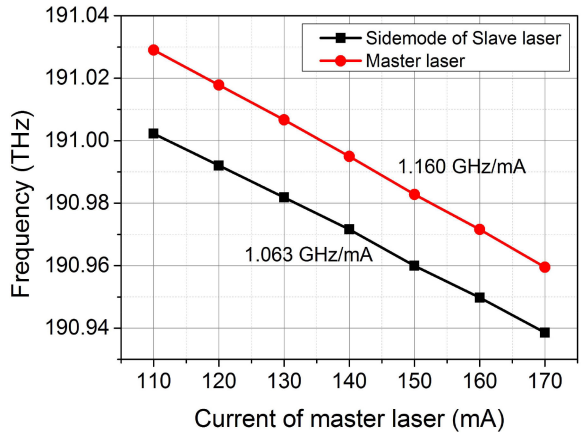

Fig. 4. Frequency of the ML and SL side-mode versus I_m.

the SL and ML are biased with different currents, the MOIL DFB laser exhibits various characteristics. Fig. 3(a) and (b) show the spectra of the SL and ML respectively when they operate independently. In order to reduce the absorption loss, a transparent current of 15 mA is injected into the SL when the ML works alone. Comparing with Fig. 3(c), when the SL and ML are biased with the same current of 50 mA, the SL and ML can operate independently and there is no interaction between them. The wavelength of the ML locates between the main mode and the side mode of the SL. From the Fig. 3(c), (d), (e) and (f), it can be seen that the wavelength of the ML has red shift due to the heating effect, when I_s is fixed at 50 mA and I_m is increased from 50 mA to 160 mA. Because of the thermal crosstalk between the ML and SL, the wavelength of the SL also drifts to the long wavelength when I_m is increased. As shown in Fig. 4, the wavelength shift rate of the ML is slightly larger than the SL. Hence, the ML wavelength shifts towards the side-mode of the SL and the higher I_m is set, the smaller detuning frequency is achieved. As a consequence, the main mode of the SL is suppressed and the side-mode is enhanced. When I_m is large enough, both modes of the SL are suppressed and SL is locked to the output of the ML section. The SL can be locked to the output of the ML with the bias current I_m from 110 mA to 160 mA [14]. It can also be seen that the frequency detuning varies from 25.78 GHz to 21.4 GHz when I_m is changed from 120 mA to 160 mA.

The output performance of the MOIL DFB laser changes significantly when it is in injection locking state. For instance, once the laser is injection locked, its linewidth reduces dramatically relative to its free-running value [24]. Fig. 5 shows the measured linewidths of the MOIL DFB laser under free running state and injection-locked state using the well-known delayed self-heterodyne technique. The linewidth of the SL is 28.2 MHz in free running state (i.e., $I_s = 50$ mA, $I_m = 0$ mA). However, its linewidth is reduced to 2.7 MHz when it is locked by the ML.

On the other hand, it has been shown both theoretically and experimentally that optical injection locking can reduce the relative intensity noise (RIN) and increase the relaxation oscillation frequency of semiconductor lasers [25]–[27]. Utilizing the method demonstrated in Ref. [28], we measured the RIN of the MOIL DFB laser with different bias currents. As

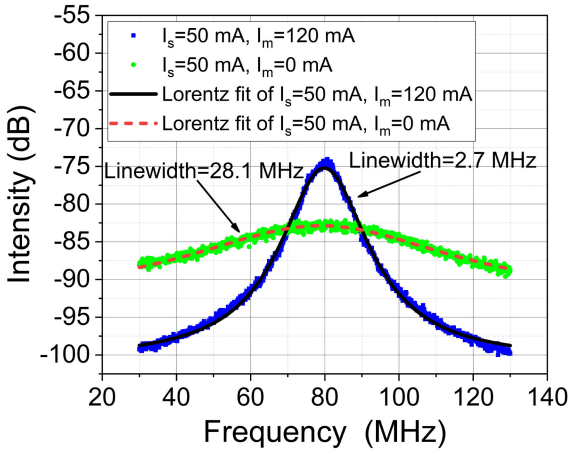

Fig. 5. Linewidth measurement of the MOIL DFB laser with different bias currents.

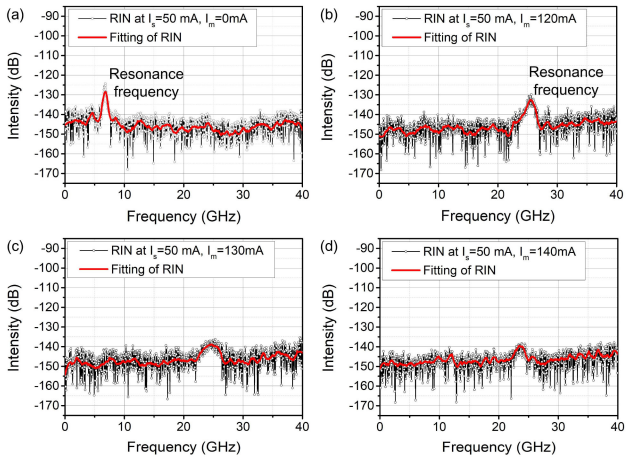

Fig. 6. The RIN of the MOIL DFB laser with $I_s = 50$ mA and (a) $I_m = 0$. (b) $I_m = 120$ mA. (c) $I_m = 130$ mA. (d) $I_m = 140$ mA.

shown in Fig. 6(a), the RIN of the MOIL DFB laser is about −124 dB/Hz in free running state. However, as shown in Fig. 6(b)–(d), the RIN is reduced significantly when the laser is in injection locked state. The RIN of the MOIL DFB laser is measured to be −139 dB/Hz with $I_s = 50$ mA and $I_m = 140$ mA, which is 15 dB lower than that of the free running state. The resonance frequencies can also be obtained in the RIN curves, which are equal to the frequency of the peak in the RIN curves. Comparing with the free running state, the resonance frequency of the MOIL DFB laser in injection locked state increases from 6 GHz to more than 25 GHz.

B. Characteristics of the SSB Modulation

The optical spectra of the MOIL DFB laser with 25-GHz RF modulation and different bias currents are shown in Fig. 7. When the MOIL DFB laser is in free-running state ($I_s = 50$ mA, $I_m = 0$ mA) with a 25-GHz RF modulation, the laser has two quasi-symmetric modulation sidebands. However, when the MOIL DFB laser is in injection-locked state ($I_s = 50$ mA, $I_m =$ 120 mA, 140 mA, 160 mA), the lower sideband is resonantly amplified by the sidemode of the SL and the upper sideband keeps

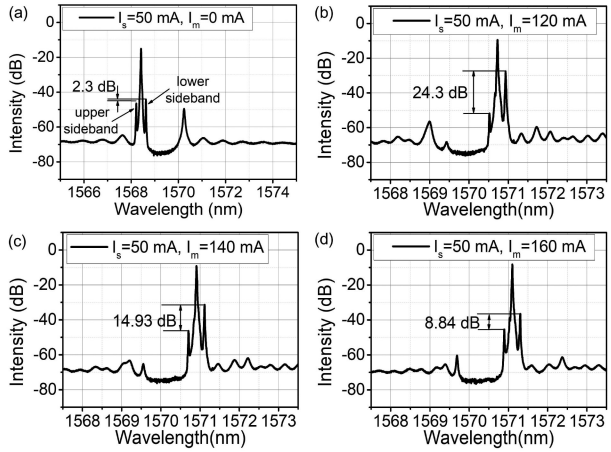

Fig. 7. The spectra of the MOIL DFB laser at different bias currents modulated by a 25-GHz RF signal.

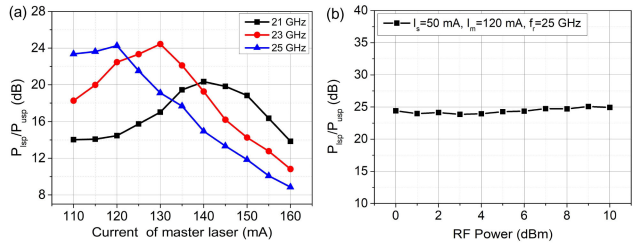

Fig. 8. (a) Measured P_{usb}/P_{lsb} value of SSB signal versus I_m with different frequency. (b) Measured P_{usb}/P_{lsb} value of SSB signal versus the RF power with $I_s = 50$ mA, $I_m = 120$ mA, and $f_r = 25$ GHz.

unchanged. Consequently, the modulation sidebands show a dramatical asymmetry. Because the frequency detuning changes with I_m, the P_{lsp}/P_{usp} varies with I_m and the maximum value of the P_{lsp}/P_{usp} occurs when the RF frequency is close to the frequency detuning.

Fig. 8(a) illustrates the relationship between the P_{lsp}/P_{usp} and I_m at different RF frequency. It is obvious that the largest P_{lsp}/P_{usp} of 21 GHz, 23 GHz and 25 GHz are observed when I_m is set at 140 mA, 130 mA and 120 mA respectively. The maximum P_{lsp}/P_{usp} for 21 GHz, 23 GHz and 25 GHz are measured to be 20.3 dB, 24.4 dB and 24.3 dB respectively. Therefore, the tunable SSB modulation at different frequency can be obtained by changing the bias currents of the MOIL DFB laser. The direct modulation will influence the stability of the injection locking process and lead to the deterioration of SSB modulation. So large injection locking range is required to achieve stable SSB modulation with high RF power. Fig. 8(b) shows the measured P_{lsp}/P_{usp} as a function of the RF power at 25 GHz when the MOIL DFB laser is biased at $I_s = 50$ mA, $I_m = 120$ mA. The P_{lsp}/P_{usp} value remains almost constant as the RF power increases from 0 dBm to 10 dBm. That is to say stable SSB modulation can be obtained utilizing the proposed method.

The fiber transmission response is a figure-of-merit for the SSB modulation, and it is defined as the ratio of the back-to-back frequency response to the frequency response after a long-distance fiber transmission [5]. Fig. 9 shows the measured

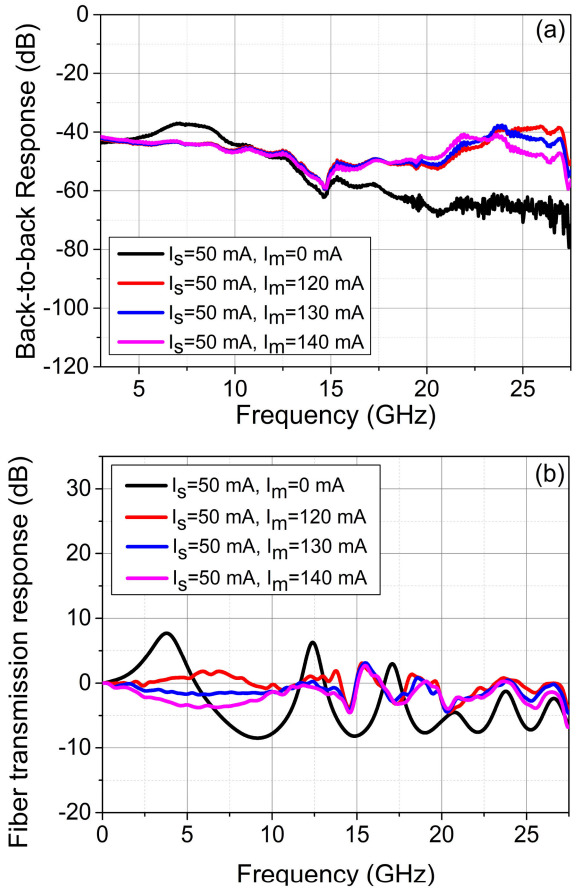

Fig. 9. (a) Measured back-to-back response of the MOIL DFB laser with different bias currents. (b) Normalized fiber transmission response of the MOIL DFB laser with different bias currents.

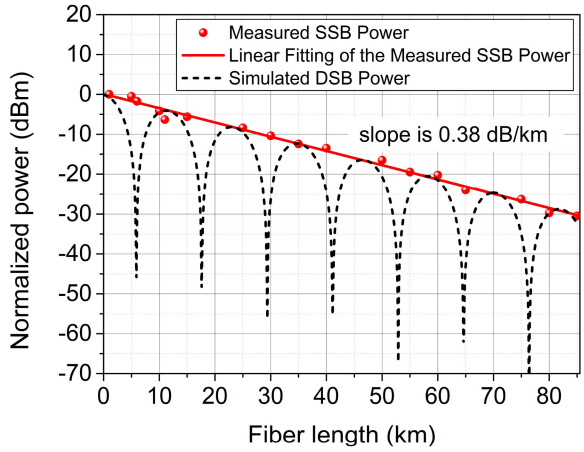

Fig. 10. Measured RF power vs fiber length. The frequency of the RF is 25 GHz. I_s and I_m are 50 mA and 120 mA, respectively.

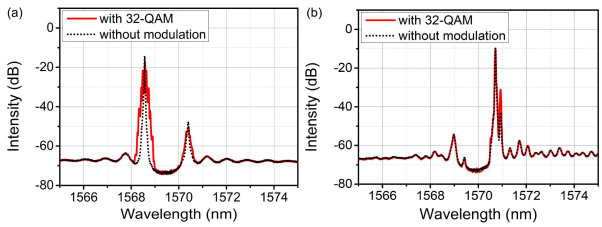

Fig. 11. Optical spectra of the MOIL DFB laser with/without the 32-QAM signals under different bias currents. (a) $I_s = 50\,\text{mA}$, $I_m = 0\,\text{mA}$. (b) $I_s = 50\,\text{mA}$, $I_m = 120\,\text{mA}$.

back-to-back response and normalized SSB fiber transmission response of the MOIL DFB laser through a 50-km SMF (the dispersion coefficient is 17 ps/nm/km). It is obvious that there is a notch near 15 GHz in the back-to-back response curve (shown in Fig. 9(a)), which is induced by the package process due to the RC time-constant-limited frequency bandwidth. The details about the back-to-back response property of the MOIL DFB laser has been discussed in [14]. Because the normalized fiber transmission response is a relative value which equals to the ratio of the back-to-back frequency response to the frequency response after 50-km fiber transmission, the notch in the back-to-back response curve does not affect the fiber transmission response shown in Fig. 9(b). As shown in Fig. 9(b), several pronounced dips are observed on the fiber transmission response curve in free-running state, which arise from the interference between the two symmetric sidebands. As a comparison, the fiber transmission response curves become much flatter when the MOIL DFB laser is in injection-locked state. The largest dip is reduced from 16.2 dB to 7.1 dB attributed to the SSB modulation.

Furthermore, in order to study the influence of the fiber chromatic dispersion on the SSB modulation signal, a 25-GHz SSB modulated RF signal is transmitted over SMFs with different lengths and the received powers of the RF signal versus the fiber lengths are shown in Fig. 10. Throughout the measurement, the MOIL DFB laser is biased at $I_s = 50\,\text{mA}$ and $I_m = 120\,\text{mA}$. Comparing with the simulated double sideband (DSB) modulation [29], there are no dips over the 85 km fiber length utilizing the proposed SSB method. The slope of the fitting line is 0.38 dB/km (i.e., the transmission loss in the fiber is about 0.19 dB/km) which agrees well with the commercial SMF loss. However, seven dips are observed in the DSB modulation case which are caused by the fiber chromatic dispersion. It is obvious that the effect of the fiber chromatic dispersion can be suppressed significantly by the generated SSB modulation.

C. Transmission Properties of the SSB Modulation

To further investigate the transmission property of the SSB modulation signal, a simple ROF link is employed utilizing the MOIL DFB laser. The SL is biased at 50 mA and directly modulated by 20 MSymbol/s 32-QAM signals with subcarriers of 21 GHz, 23 GHz and 25 GHz respectively. The signals from the laser are transmitted through a 25-km SMF and detected by the 50-GHz photodetector. Then the received signals are analyzed by the ESA.

The optical spectra of the MOIL DFB laser modulated by the 32-QAM signals under different bias currents are shown in Fig. 11. As a comparison the optical spectra without modulation are also illustrated in Fig. 11. Fig. 11(a) illustrates that the optical spectrum of the MOIL DFB laser is broadened significantly by the modulation of the 32-QAM signal when it is in free running

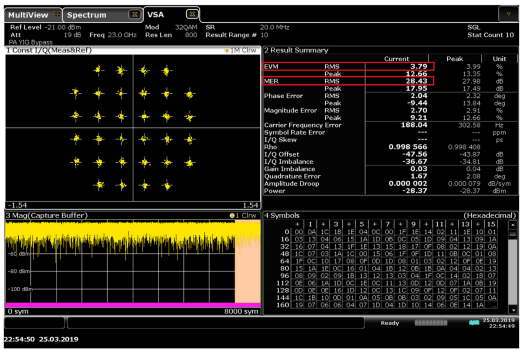

Fig. 12 The constellation diagram and analyzed results obtained from the ESA.

state. However, the 32-QAM signal has little effect on the optical spectrum when the MOIL DFB laser is injection locked. In other words, the injection locking method can effectively reduce the modulation chirp, resulting in smaller signal distortion.

Fig. 12 shows the constellation diagram of the received signal of 32-QAM with 23-GHz subcarrier when the MOIL DFB laser is under bias currents of $I_s = 50$ mA, $I_m = 130$ mA. The EVM and modulation error ratio (MER) can also be obtained from the analyzed results. Fig. 13 shows the measured EVMs back-to-back and after 25 km fiber transmission of the link versus received optical power at different bias currents. It can be seen that the optimum EVM of the signal with 21 GHz subcarrier after 25 km fiber transmission is obtained when the ML is biased at 140 mA. However, the optimum EVMs for 23 GHz and 25 GHz appear when the ML is biased at 130 mA and 120 mA. Comparing with the measured results of Fig. 8, it is obvious that the optimum EVMs are achieved when the MOIL DFB laser is biased to obtain the largest P_{lsp}/P_{usp}.

It is well known that, the BER of the link can be calculated from the measured MER and the relationship between the BER and MER for m-QAM signal is determined by the following equation [30]:

$$BER = \frac{2\left(1-\frac{1}{\sqrt{m}}\right)\cdot erfc\sqrt{\frac{2MER}{(2m-2)}}}{\log_2(m)} \quad (1)$$

where *erfc* is the complementary error function.

Fig. 14 shows the calculated BERs of the 32-QAM signal with 23-GHz subcarrier from the measured MERs which are shown in Table I. The optimized BER less than 10^{-13} after 25-km transmission is observed. The BERs after 25 km transmission exhibit power penalty compared with the back-to-back case, which is caused by the residue fiber chromatic dispersion effect from the upper sideband. Fortunately, the power penalty can also be reduced obviously by tuning the bias current of the MOIL DFB laser. Fig. 15 shows the optimized BERs of the link with subcarrier of 21 GHz, 23 GHz and 25 GHz. It is obvious that BERs less than 10^{-9} with different subcarriers can be achieved by tuning the bias current of the MOIL DFB laser.

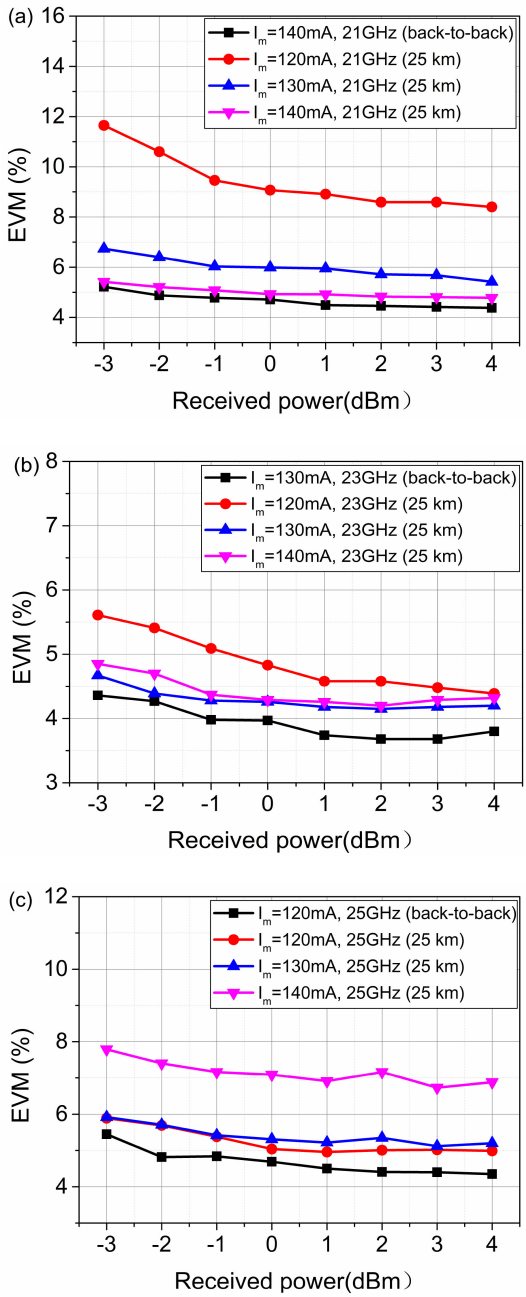

Fig. 13. The measured EVMs versus the received optical powers with different biase currents. (a) Subcarrier frequency is 21 GHz. (b) Subcarrier frequency is 23 GHz. (c) Subcarrier frequency is 25 GHz.

TABLE I
MEASURED MER FOR 32-QAM 23 GHZ SIGNAL WITH DIFFERENT RECEIVED OPTICAL POWER

Received power (dBm)	Back-to-Back I_m=130 mA	25 km I_m=120 mA	25 km I_m=130 mA	25 km I_m=140 mA
-3	527.2299	317.6874	459.1980	424.6196
-2	547.0160	341.1929	530.8844	451.8559
-1	629.5062	385.4784	545.7579	522.3962
0	635.3309	429.5364	550.8077	543.2503
1	714.4963	476.4310	571.4786	550.8077
2	739.6053	476.4309	582.1032	567.5446

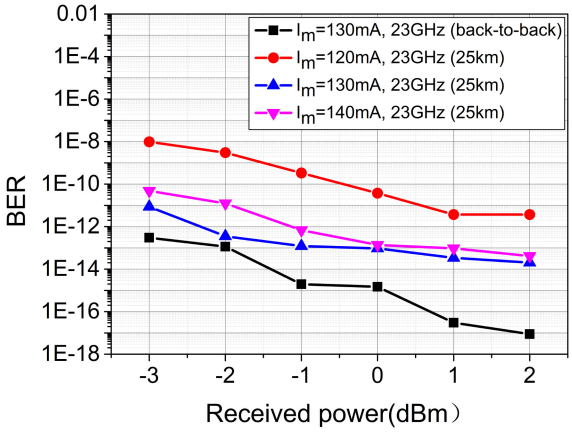

Fig. 14. The calculated BER from the measured MER of the ROF link with 23-GHz subcarrier.

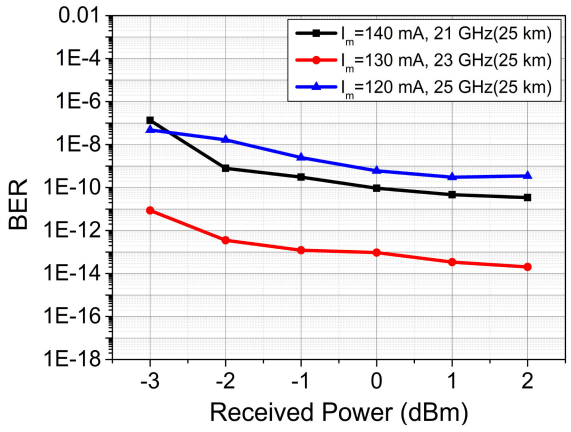

Fig. 15. The calculated BER from the measured MER of the ROF link with subcarrier of 21 GHz, 23 GHz, and 25 GHz at different bias currents.

IV. Conclusion

A method to realize SSB modulation has been experimentally demonstrated utilizing the MOIL DFB laser for the first time. The asymmetric modulation sidebands can be obtained by tuning the bias currents of the ML and SL. The maximum P_{lsp}/P_{usp} is measured to be 24.4 dB. The fiber transmission response of SSB modulation is much flatter than the DSB modulation. The dips in the fiber transmission response curve are reduced by 9.1 dB. 20 MSymbol/s 32-QAM signals with 21 GHz, 23 GHz and 25 GHz subcarriers are transmitted through 25-km SMF. The optimum EVMs are achieved when the SSB modulation with the largest P_{lsp}/P_{usp}. is generated. The BER of the link less than 10^{-13} is observed. The effect of fiber chromatic dispersion is suppressed dramatically using the proposed method.

References

[1] G. H. Smith, D. Novak, and Z. Ahmed, "Overcoming chromatic-dispersion effects in fiber-wireless systems incorporating external modulators," *IEEE Trans. Microw. Theory Tech.*, vol. 45, no. 8, pp. 1410–1415, Aug. 1997.

[2] Y. Ogiso, Y. Tsuchiya, S. Shinada, S. Nakajima, T. Kawanishi, and H. Nakajima, "High extinction-ratio integrated Mach–Zehnder modulator with active Y-branch for optical SSB signal generation," *IEEE Photon. Technol. Lett.*, vol. 22, no. 12, pp. 941–943, Jun. 2010.

[3] Y. C. Shen, X. M. Zhang, and K. S. Chen, "Optical single sideband modulation of 11-GHz RoF system using stimulated Brillouin scattering," *IEEE Photon. Technol. Lett.*, vol. 17, no. 6, pp. 1277–1279, Jun. 2005.

[4] J. Yu, M. Huang, Z. Jia, T. Wang, and G. Chang, "A novel scheme to generate single-sideband millimeter-wave signals by using low-frequency local oscillator signal," *IEEE Photon. Technol. Lett.*, vol. 20, no. 7, pp. 478–480, Apr. 2008.

[5] H. K. Sung, E. K. Lau, and M. C. Wu, "Optical single sideband modulation using strong optical injection-locked semiconductor lasers," *IEEE Photon. Technol. Lett.*, vol. 19, no. 13, pp. 1005–1007, Jul. 2007.

[6] J. T. Xiong *et al.*, "A novel approach to realizing SSB modulation with optimum optical carrier to sideband ratio," *IEEE Photon. Technol. Lett.*, vol. 25, no. 12, pp. 1114–1117, Jun. 2013.

[7] A. Tauke-Pedretti *et al.*, "Mutual injection locking of monolithically integrated coupled-cavity DBR lasers," *IEEE Photon. Technol. Lett.*, vol. 23, no. 13, pp. 908–910, Jul. 2011.

[8] C. Sun *et al.*, "Modulation characteristics enhancement of monolithically integrated laser diodes under mutual injection locking," *IEEE J. Quantum Electron.*, vol. 21, no. 6, pp. 628–635, Nov.–Dec. 2015.

[9] P. M. Anandarajah *et al.*, "Integrated two-section discrete mode laser," *IEEE Photon. J.*, vol. 4, no. 6, pp. 2085–2094, Dec. 2012.

[10] D. Liu, C. Sun, B. Xiong, and Y. Luo, "Suppression of chaos in integrated twin DFB lasers for millimeter-wave generation," *Opt. Exp.*, vol. 21, pp. 2444–2451, 2013.

[11] X. Q. Qi, L. Xie, and Y. Liu, "Comparisons of typical nonlinear states in single- and dual-beam optically injected semiconductor lasers," *Opt. Commun.*, vol. 309, pp. 163–169, 2013.

[12] R. Diaz, S. C. Chan, and J. M. Liu, "Lidar detection using a dual-frequency source," *Opt. Lett.*, vol. 31, pp. 3600–3602, 2006.

[13] J. Li *et al.*, "Photonic generation of linearly chirped microwave waveforms using a monolithic integrated three-section laser," *Opt. Exp.*, vol. 26, pp. 9676–9685, 2018.

[14] Y. S. Zhang *et al.*, "Modulation properties enhancement in a monolithic integrated two-section DFB laser utilizing side-mode injection locking method," *Opt. Exp.*, vol. 25, pp. 27595–27608, 2017.

[15] J. H. Seo, Y. K. Seo, and W. Y. Choi, "Nonlinear distortion suppression in directly modulated DFB lasers by side-mode optical injection," in *Proc. IEEE MTT-S Int. Microw. Symp. Digest*, 2001, pp. 555–558.

[16] J. M. Luo and M. Osinski, "Comparison of side-mode and peak-mode injection locking characteristics of semiconductor lasers," in *Proc. LEOS'92 Conf.*, 1992, pp. 94–95.

[17] W. W. Chow, Z. S. Yang, G. A. Vawter, and E. J. Skogen, "Modulation response improvement with isolator-free injection-locking," *IEEE Photon. Technol. Lett.*, vol. 21, no. 13, pp. 839–841, Jul. 2009.

[18] S. Noda, K. Kojima, and K. Kyuma, "Mutual injection-locking properties of monolithically-integrated surface-emitting multiple-quantum-well distributed feedback lasers," *IEEE J. Quantum Electron.*, vol. 26, no. 11, pp. 1883–1894, Nov. 1990.

[19] C. Browning *et al.*, "Performance improvement of 10 Gb/s direct modulation OFDM by optical injection using monolithically integrated discrete mode lasers," *Opt. Exp.*, vol. 19, pp. B289–B294, 2011.

[20] A. Tauke-Pedretti *et al.*, "Mutual injection locking of monolithically integrated coupled-cavity DBR lasers," *IEEE Photon. Technol. Lett.*, vol. 23, no. 13, pp. 908–910, Jul. 2011.

[21] H. K. Sung *et al.*, "Modulation bandwidth enhancement and nonlinear distortion suppression in directly modulated monolithic injection-locked DFB lasers," in *Proc. Int. Topical Meet. Microw. Photon.*, IEEE, 2003, pp. 27–30.

[22] C. Sun *et al.*, "Modulation characteristics enhancement of monolithically integrated laser diodes under mutual injection locking," *IEEE. J. Sel. Top. Quantum Electron.* vol. 21, no. 6, pp. 628–635, Nov.–Dec. 2015.

[23] H.-K. Sung *et al.*, "Modulation bandwidth enhancement and nonlinear distortion suppression in directly modulated monolithic injection-locked DFB lasers," in *Proc. Int. Topical Meet. Microw. Photon.*, MWP, 2003, pp. 27–30.

[24] A. Takada and W. Imajuku, "Linewidth narrowing and optical phase control of mode-locked semiconductor laser employing optical injection locking," *IEEE Photon. Technol. Lett.*, vol. 9, no. 10, pp. 1328–1330, Oct. 1997.

[25] X. Jin and S. L. Chuang, "Relative intensity noise characteristics of injection-locked semiconductor lasers," *Appl. Phys. Lett.*, vol. 77, pp. 1250–1252, 2000.

[26] G. Yabre, H. De Waardt, H. P. A. van den Boom, and G. Khoe, "Noise characteristics of single-mode semiconductor lasers under external light injection," *IEEE J. Quantum Electron.*, vol. 36, no. 3, pp. 385–393, Mar. 2000.

[27] J. M. Liu, H. F. Chen, X. J. Meng, and T. B. Simpson, "Modulation bandwidth, noise and stability of a semiconductor laser subject to strong injection locking," *IEEE Photon. Technol. Lett.*, vol. 9, no. 10, pp. 1325–1327, Oct. 1997.
[28] P. Anandarajah, S. Latkowski, C. Browning, R. Zhou, J. O'Carroll, and R. Phelan, "Integrated two-section discrete mode laser," *IEEE Photonics J.*, vol. 4, no. 6, pp. 2085–2094, Dec. 2012.
[29] G. H. Smith, D. Novak, and Z. Ahmed, "Overcoming chromatic dispersion effects in fiber-wireless systems incorporating external modulators," *IEEE Trans. Microw. Theory Tech.*, vol. 45, no. 8, pp. 1410–1415, Aug. 1997.
[30] V. J. Urick, J. X. Qiu, and F. Bucholtz, "Wide-band QAM-over-fiber using phase modulation and interferometric demodulation," *IEEE Photon. Technol. Lett.*, vol. 16, no. 10, pp. 2374–2376, Oct. 2004.

Yunshan Zhang received the B.S. degree in science and technology of electronics from Shandong University, Jinan, Shandong, China, in 2002 and the Ph.D. degree in physical electronics from the Beijing Institute of Technology, Beijing, China, 2011. Currently, he is a Postdoctor with the College of Engineering and Applied Sciences, Nanjing University, Nanjing, China majoring in the design of DFB lasers and laser arrays. His research interests include solid state lasers, DFB semiconductor lasers, fiber communication and photonic integrated circuits.

Bocheng Yuan received the B.S. degree from the College of Electronic and Optical Engineering and College of Microelectronics, Nanjing University of Posts and Telecommunications, Nanjing, Jiangsu, China, in 2018. He is currently working toward the master's degree with the College of Electronics, Optical Engineering and Microelectronics, Nanjing University of Posts and Telecommunications, Nanjing. His research interests include DFB semiconductor lasers and fiber communication system. He is engaged in the design and testing of DFB laser chips.

Lianyan Li received the B.S. and Ph.D. degrees from the College of Engineering and Applied Sciences, Nanjing University, Nanjing, China, in 2011 and 2015, respectively. Currently, she is a Lecturer with the Nanjing University of Posts and Telecommunications, Nanjing, Jiangsu, China. Her research interests include tunable semiconductor lasers, photonic integrated circuits, and silicon photonics.

Jie Zeng, biography not available at the time of publication.

Zijun Shang was born in April, 1998. She has been working toward the degree majoring in telecommunication engineering and management with the Nanjing University of Posts and Telecommunications, Nanjing, China, since 2016.

Jilin Zheng received the B.S. degree and the PhD. degree in electromagnetic field and microwave technology from the PLA University of Science and Technology, Nanjing, China, in 2005 and 2010, respectively. His research interests include microwave-photonics, DFB semiconductor lasers, fiber communication, and photonic integrated circuits. Currently, he is majoring in advanced DFB lasers and their applications.

Zuye Lu, biography not available at the time of publication.

Shijian Guan was born in 1997. He received the bachelor's degree in optoelectronics information science and engineering from Nanjing University, Nanjing, Jiangsu, China, in 2019 where he is currently working toward graduation majoring in quantum electronics and optical engineering.

Xing Zhang was born in Jilin, China, in 1983. He received the B.S. degree in electronics from Jilin University, Jilin, China, in 2005, and the Ph.D. degree in condensed matter physics from the Changchun Institute of Optics, Fine Mechanics and Physics, Chinese Academy of Sciences (CAS), Beijing, China, in 2011. In 2011, he joined the Changchun Institute of Optics, Fine Mechanics and Physics, CAS, Beijing, where he is currently an Associate Research Fellow. His current research interests include the power scaling of VCSELs and high power LDs.

Rulei Xiao received the B.S. degree in material physics and the Ph.D. degree in optical engineering from Nanjing University, Nanjing, China, in 2014 and 2019, respectively. He is currently an Associate Research Fellow with the College of Engineering and Applied Science, Nanjing University. His research interests include tunable semiconductor laser and multiwavelength laser array.

Tao Fang received the doctoral degree in electromagnetic field and microwave technology in 2008 from the PLA University of Science and Technology, Beijing, China. Currently, he is a Research Fellow with the College of Engineering and Applied Sciences, Nanjing University, Nanjing, China. His research interests include high speed optical communications, semiconductor laser and tunable lasers, microwave photonics, and photonic integrated circuits.

Yuechun Shi received the doctoral degree in electromagnetic field and microwave technology from Nanjing University, Nanjing, China, in 2012. From 2012 to 2013, he studied in Royal Institute of Technology (KTH), Stockholm, Sweden, as a Visiting Researcher. Currently, he is a Research Associate with the College of Engineering and Applied Sciences, Nanjing University. His research interests include DFB semiconductor laser and laser array, passive waveguide filters, photonic integrated circuits, and high speed optical communications.

Hui Zou received the doctoral degree in communication and information systems from Beijing Jiaotong University, Beijing, China, in 2014. Currently, he is an Associate Professor with the College of Electronic and Optical Engineering, Nanjing University of Posts and Telecommunications, Nanjing, Jiangsu, China. His research interests include design of special optical fiber devices and photoelectric signal processing technology.

Jianping Shen received the doctoral degree in optical engineering from Beijing Jiaotong University, Beijing, China, in 2015. Currently, he is a Teacher with the College of Electronic and Optical Engineering and College of Microelectronics, Nanjing University of Posts and Telecommunications, Nanjing, Jiangsu, China. His research interests include DPSSL, optical waveguide, semiconductor laser, and laser applications.

Xiangfei Chen received the B.S. degree in physics, from the Soochow University, Suzhou, China, in 1991, and the M.S. and Ph.D. degrees in physics from the Nanjing University, Nanjing, China, in 1993 and 1996, respectively. From 1996 to 2000, he was a Faculty Member with Nanjing University of Post and Telecommunication Technology, Nanjing, Jiangsu, China. From 2000 to 2006, he served as an Associate Professor with the Department of Electrical Engineering, Tsinghua University, Beijing, China. From October 2004 to April 2005, he was a Visiting Scholar with Microwave Photonics Research Laboratory, School of Information Technology and Engineering, University of Ottawa, Ottawa, ON, Canada. He is currently a Professor with Microwave Photonics Technology Laboratory, National Laboratory of Microstructures and College of Engineering and Applied Sciences, Nanjing University. He has authored or coauthored more than 70 research papers. He holds a number of patents. His research interests include development of novel optical devices for high-speed large-capacity optical networks, microwave photonic systems, and fiber-optic sensors.

Dr. Chen is a Member of the Optical Society of American (OSA).